X-ray diffraction characterization of multilayer semiconductor structures*

Thad Vreeland, Jr. and Bruce M. Paine
Division of Engineering and Applied Science, California Institute of Technology, Pasadena, California 91125

(Received 11 April 1986; accepted 23 May 1986)

The analysis of double-crystal x-ray rocking curves of single-crystal layered structures can give valuable information on layer strains, displacement of atoms from normal lattice sites (which reduces the structure factor), crystallographic misorientations, and crystal defects. Both strains and misorientations cause shifts in the Bragg angle. These two effects are readily separated using two or more rocking curves with appropriate *hkl* reflections. The thickness of a layer and its structure factor affect the integrated intensity of a shifted Bragg peak while the width of the peak is affected by the thickness of the layer and its defect content. Calculation of the x-ray rocking curve of a crystal with strain, structure factor, and damage (displaced atoms) is done using the kinematical or single-scattering theory for thin layers or the dynamical theory for thick strongly diffracting layers. The problem of uniqueness of the rocking curve calculated for a given structure is discussed. Application of the rocking curve technique to the characterization of multilayer semiconductor structures is presented. The applications include Si homoepitaxy and heteroepitaxy, metal silicide on Si, GaAs implanted with 0.3–15 MeV ions, quaternary compound laser structures, AlGaAs/GaAs and HgCdTe/CdTe superlattices, and strains in polycrystalline or noncrystalline films on a thin single crystal.

I. INTRODUCTION

Recent improvements in methods of crystal growth have led to the production of epitaxial layers and superlattices of nearly perfect crystallinity. The free lattice parameters of the epilayer and substrate or of the alternating layers of a superlattice are usually unequal, so that the modulation of the composition results in a modulated strain. The physical properties of these devices depend on the state of strain as well as the composition modulation, which makes possible the design of devices with novel features.

Progress in this highly relevant and promising new field is determined not only by improvements in crystal growth techniques, but also by the ability to characterize superlattices and other layered structures easily and accurately. Among the analytical techniques that can be applied, the nondestructive ones are of particular value. Of these, double-crystal x-ray diffractometry is emerging as the leading technique with which to obtain structural information on superlattices, epitaxial layers, and ion irradiated crystals. The reason is that this technique can provide quantitative depth profiles of the strain (and hence the composition of epitaxial layers) for a structure analyzed. It does so with ease and accuracy for epilayers and superlattices of any type (insulators, semiconductors, metals). Under optimum conditions, x-ray diffraction is capable of detecting strains of $< 10^{-8}$ in single crystals.[1] Strains which cause a change in the Bragg angle for x-ray diffraction may be determined quantitatively from a plot of the diffracted x-ray intensity normalized to the incident x-ray intensity (the reflecting power) versus deviation of angle from the Bragg peak of an unstrained crystal. This plot, the x-ray rocking curve for a chosen reflection and incident plane-wave radiation, is called the x-ray rocking curve. In comparison with other analytical equipment capable of providing depth profiles (e.g., Auger electron spectrometry, secondary ion mass spectrometry, or backscattering spectrometry), double-crystal x-ray diffractometers are quite inexpensive and simple. Because of these advantages in cost, performance, and versatility, x-ray rocking curves will no doubt become a standard analytical tool for laboratories involved in the growth of epitaxial structures and superlattices.

The theoretical framework for calculating x-ray wave fields in crystals is well established. Treatments of the diffraction of plane waves in uniform crystal layers, using the kinematical approximation (valid for weakly diffracting layers where multiple scattering can be ignored),[2] or the dynamical theory[3] (which takes into account multiple scattering and anomalous absorption) permit quantitative prediction of the rocking curve for a crystal with epilayers whose strain and damage are known. The following section gives a description of a double-crystal rocking curve system in which a highly perfect first crystal is employed to obtain a good approximation to a plane monochromatic wave, and the second crystal is the sample to be analyzed. The next section describes briefly the procedure for analysis of the rocking curves. Then examples of the application of the rocking curve system to the characterization of a number of semiconductor structures are given in the last section of the paper.

II. THE DOUBLE-CRYSTAL DIFFRACTOMETER SYSTEM

A system for obtaining rocking curves from a single-crystal sample consists of (a) x-ray source (conventional electron-bombarded metal target sources are most commonly employed), (b) a monochromater (to select a monochromatic plane wave from the broadband spherical wave source), (c) slits placed between monochromater and sample, (d) the diffractometer (Bragg angle drive with sample stage), (e) x-ray detector to measure intensity of incident and diffracted x rays, and (f) means for system control and recording and display of rocking curves. A schematic dia-

*This paper was chosen from the symposium on Thin Films for Microelectronics to receive the Bunshah Award.

 0734-2101/86/063153-07$01.00

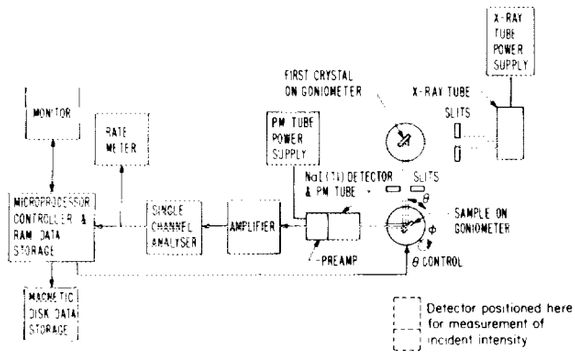

FIG. 1. Schematic of a microprocessor-controlled double-crystal rocking curve system.

gram of the system designed and built at Caltech is shown in Fig. 1. The x-ray source is the conventional sealed-tube type. Single-crystal surfaces of high quality (preferably dislocation-free crystals) are used in the monochromater, typically (100) or (111) surfaces of Si, Ge, or GaAs. A highly effective monochromater, which utilizes four surfaces on two channel-cut crystals, has been described by Bartels.[4] A single-surface monochromater is more commonly employed as shown in Fig. 1. This monochromater passes both $K_{\alpha 1}$ and $K_{\alpha 2}$ x-ray wavelengths, and when the Bragg angle of the sample crystal differs from that of the monochromater crystal (dispersive setting), the slits are adjusted to eliminate the weaker $K_{\alpha 2}$. The slits also serve to limit the area to be examined on the second crystal.

Our diffractometer resolves angular changes of $\sim 0.0001°$; this is suitable for most applications. Step-scanning capability is desirable if an automated digital data acquisition system is to be used. A step-scan range of $\pm$ 1.5° is adequate for most applications. A sample stage on the diffractometer, which permits the sample surface to be located so as to contain the axis for Bragg angle adjustment, should also permit sample translation along one or two axes in the sample surface and rotation about an axis normal to the sample surface. The x-ray detector employed in our system uses a NaI(Tl) crystal with a 0.13-mm-thick Be window and a photomultiplier tube with preamplifier. Detector signals are processed in a single-channel analyzer. A rate meter is useful in manual system alignment. Diffractometer scans are programmed and stored using a Radix data acquisition system. Rocking curve data are transferred from the Radix system to a microcomputer for nonvolatile (disk) storage, plotting, and analysis.

III. ANALYSIS OF THE ROCKING CURVE

Single epitaxial layers are readily analyzed for strain, thickness, and crystal quality by employing an iterative process in which a calculated rocking curve is fitted to the measured curve. Layers whose reflecting power is less than about 6% are analyzed using the kinematical theory,[2] while more strongly diffracting layers are analyzed using the dynamical theory (see, e.g., Ref. 5). Since most diffractometers used in the rocking curve technique do not give absolute angle information, relative angles from a reference Bragg peak are used. An epilayer substrate usually provides a reference Bragg peak. Strains in the layer, relative to the strains in the reference crystal, are determined from the angular shift in Bragg peak of the layer relative to the Bragg peak of the reference as discussed below. In general, the normal strains (as opposed to shear strains) will be measured. For the usual case of thin epilayers on relatively thick substrates, the substrate stress and strain are essentially zero. In the case of homoepitaxy, the x-ray strains (defined as strains relative to the substrate rather than to the unstressed layer) are equal to the strains in elasticity theory. When the epilayer has a different free lattice parameter from the substrate, the elasticity strains (normal strains) are related to the x-ray strains by

$$\epsilon_{\text{elasticity}} = (\epsilon_{\text{x ray}} + \epsilon_0)/(1 - \epsilon_0) \cong \epsilon_{\text{x ray}} + \epsilon_0 , \quad (1)$$

where $\epsilon_0 = 1 - d_{\text{free}}/d_{\text{sub}}$, d_{free} = plane spacing of a stress-free layer in the direction of the strain, and d_{sub} = plane spacing of the substrate in the direction of the strain. The free lattice parameters of substitutional solid solutions of semiconductor materials follow Vegard's law (i.e., are linear with concentration of solute), so that the solute concentration in the epilayer may be calculated from the x-ray strains and lattice parameters (and the elastic constants) of the elemental or compound semiconductors.

The principal strain perpendicular to the layer surface (perpendicular strain) is determined directly from a rocking curve from diffraction planes which are nominally parallel to the layer surface (symmetric diffraction). The angular shift in the Bragg peak from the layer with respect to the Bragg peak from the reference crystal, is given by

$$-\Delta\theta = (\Delta d/d_{\text{sub}})\tan\theta_B \pm \xi \quad \text{(symmetric diffraction)}, \quad (2)$$

where $\Delta d/d_{\text{sub}}$ = the perpendicular x-ray strain, θ_B = substrate Bragg angle, and ξ = component in the diffraction plane of the misorientation angle between the layer and the reference crystal. θ is measured from the diffracting plane to the incident x-ray vector. The sign of ξ reverses when incident and diffracted beam directions are reversed. When $\xi = 0$, the $\Delta\theta$ for a single, prominent shifted peak in the rocking curve gives the average strain in the layer. The use of two rocking curves, with the diffraction vectors reversed, permits determination of the $\Delta d/d_{\text{sub}}$ and ξ.[7]

Equation (2) is modified for asymmetric rocking curves[8] when a layer has both perpendicular ($\epsilon^{\perp}$) and parallel ($\epsilon^{\parallel}$) x-ray strains. Parallel strains in an epilayer imply loss of coherency and misfit dislocations. Let ψ be the angle between the diffracting plane and the layer surface. The Bragg angle shift due to strain and misorientation is then

$$-\Delta\theta = k_1\epsilon^{\perp} + k_2\epsilon^{\parallel} \pm \xi, \quad (3)$$

where

$$k_1 = \cos^2\psi \tan\theta_B \pm \sin\psi\cos\psi, \quad (4)$$

$$k_2 = \sin^2\psi \tan\theta_B \mp \sin\psi\cos\psi. \quad (5)$$

The upper sign in the last term of Eqs. (3)–(5) is used when the angle of x-ray incidence with respect to the surface is $\theta_B - \psi$ and the lower sign is used when it is $\theta_B + \psi$. The first term in Eqs. (4) and (5) gives the contribution from $\Delta d/d$ and the second term gives the contribution from strain-induced rotation of the Bragg planes. Equation (3) reduces to Eq. (2) for the symmetric ($\psi = 0$) case. The perpendicular strain is usually determined directly from the symmetric rocking curve (or from two symmetric rocking curves with

diffraction vectors reversed when $\xi \neq 0$). The parallel strains are then found from the peak shift in asymmetric rocking curves using Eq. (3).

A quantitative prediction of the rocking curve which gives peak amplitudes as well as angular shifts for weakly diffracting layers (reflecting power $<6\%$) has been given by Speriosu.[2] When there are strain gradients, the actual strain distribution may be approximated by a number of discrete layers each with constant strain. The diffracted intensity is calculated from the sum of wave fields from the layers (taking account of phase and normal absorption). The layer approximation for strongly diffracting layers has been developed using dynamical theory by several authors (see e.g., Ref. 5).

Plane-wave rocking curves are calculated assuming monochromatic radiation and perfect first and second crystals. The experimental rocking curves are broadened due to imperfections in the crystals, and a small x-ray divergence and wavelength spread. For highly perfect first and second crystals, this broadening produces the equivalent of a convolution of the plane-wave rocking curve with a Gaussian having a standard deviation of ~ 10 arcsec. Crystal defects in epitaxial layers cause further broadening of the rocking curve. It is possible to distinguish between rocking curve broadening due to a particle size effect (dislocation substructure) and deformation broadening due to randomly distributed dislocations.[6] Energetic irradiation produces point defects in crystals which remove atoms from normal lattice sites. This reduces the structure factor, and in the limit reduces the diffracted intensity to zero when the crystal is rendered amorphous. This damage may be taken into account in calculating a rocking curve.[2]

A. Uniqueness of the strain and damage profiles

The rocking curve calculated for a given number of layers each with specified structure, strains, and damage is unique. The converse, however, is not true. A given experimental rocking curve can be fit with calculated curves based on different depth profiles of strain and damage. This is due in part to the insensitivity of the calculated curve to the depth of a diffracting layer when normal absorption is small (the layers in a given profile can then be interchanged with little effect on the calculated curve). Small incident x-ray angles may be used to distinguish whether a strained layer is near the surface or not. In the majority of cases, sufficient information is available on the preparation or treatment of the sample to limit the range of strained layer thicknesses and damage which must be considered (number of epilayers and their approximate thickness, ion energy deposited in nuclear collisions, etc.). Calculation of rocking curves for strain and damage distributions which fall within this limited range generally results in only one good fit to the experimental curve, and the distribution which gives this fit may be safely assumed to approximate the actual distribution.

IV. APPLICATIONS

Experimental rocking curves obtained from a variety of layered semiconductor structures are reviewed in this section. In some cases only the peak shifts are analyzed to give average strains in the layers. In other cases, depth profiles of strain (or strain and damage) are obtained by iterative fitting of calculated curves to the experimental rocking curves.

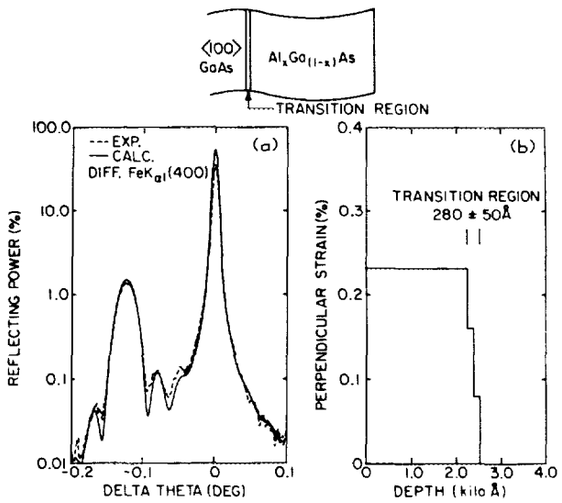

FIG. 2. (a) Symmetric (400) rocking curve for a MOCVD $Al_xGa_{1-x}As$ epilayer on GaAs obtained using Fe $K_{\alpha 1}$ (dashed curve) and the calculated (solid) curve using the perpendicular x-ray strain profile shown in (b).

A. Heteroepitaxial layers: $Al_xGa_{1-x}As$ on GaAs and $CoSi_2$ on Si

Growth of thin layers of $Al_xGa_{1-x}As$ on a relatively thick GaAs substrate by metal organic chemical vapor deposition (MOCVD) produces a structure with compressive strains in the plane of the epilayer on a substrate which is essentially stress-free ($d_{free} > d_{sub}$). A Poisson's strain perpendicular to the surface results, and this strain together with the change in d due to the alloying causes the Bragg peak from planes nominally parallel to the layer surface to be shifted from the Bragg peak of the substrate [Eq. (2)]. A symmetric rocking curve from a MOCVD sample is shown as a dashed curve in Fig. 2(a).[9] The solid curve in the figure was calculated (using kinematical theory) for the x-ray strain shown in Fig. 2(b). The layer thicknesses and strains were adjusted to give good agreement between the calculated and experimental curves. A good fit cannot be obtained for a single, constant strain layer, which shows the epilayer was grown with an Al content that varied with depth. Asymmetric rocking curves show that the parallel strain is zero in the as-grown AlGaAs epilayers (i.e., there is no loss of coherency with the GaAs substrate).

A $CoSi_2$ epilayer on (111) Si was characterized using the rocking curve technique.[10] Figure 3(a) shows an experimental Fe $K_{\alpha 1}$ symmetric (111) rocking curve and Fig. 3(b) shows the asymmetric (331) rocking curve. Average perpendicular and parallel x-ray strains were calculated from the $\Delta\theta$ values in Figs. 3(a) and 3(b) (-2.08% and -0.11%, respectively). The rocking curves were found to readily distinguish between $CoSi_2$ layers with different crystal quality by the breadth of the layer peaks. Ion channeling studies did not resolve any difference.

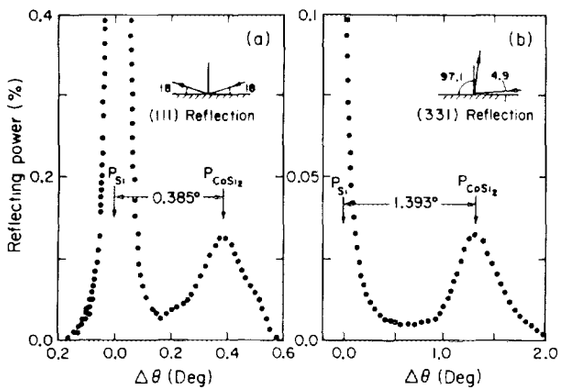

FIG. 3. (a) Symmetric Fe $K_{\alpha 1}$ (111) rocking curve for a single layer of $CoSi_2$ on (111) Si grown by electron gun evaporation (Ref. 10). (b) Asymmetric Fe $K_{\alpha 1}$ (331) rocking curve for the layer.

B. Si on sapphire

Perpendicular and parallel strains were measured in a heteroepitaxial (001) Si layer grown on $(1\bar{1}02)$ sapphire.[11] The measurement of parallel strains requires the use of asymmetric rocking curves. In this study, a stress-free Si reference crystal was fixed to the epilayer (with crystallographic alignment $\sim 1°$). The x rays were simultaneously diffracted from the layer and the reference crystal and peak shifts using symmetric rocking curves and rocking curves from equivalent asymmetric planes were used to determine the strains. Figure 4 shows a pair of superimposed (004) rocking curves obtained using the technique of reversing the diffraction vectors. The reference crystal peak is at $\Delta\theta = 0$. One-half of the sum of the peak shifts divided by $\tan\theta_B$ gives the perpendicular strain (0.303%) while one-half of the difference gives ξ. The strains determined using the stress-free Si crystal are elasticity strains ($\epsilon_0 = 0$). Analysis of the epilayer peak broadening gives information on the defect content of the layer.

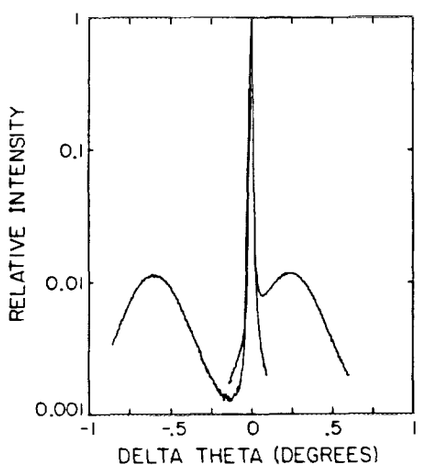

FIG. 4. Pair of superimposed symmetric (004) rocking curves from an (001) Si epilayer on (1102) sapphire with an (001) Si reference crystal on the layer surface, using Fe $K_{\alpha 1}$ radiation (Ref. 11). The peaks at $\Delta\theta = 0$ are from the reference crystal. Analysis of the $\Delta\theta$ values for the two rocking curves (taken with diffraction vectors reversed) gives the perpendicular strain in the layer and the component of misorientation angle between the layer and the reference crystal.

C. Quaternary laser structures

Compounds of InGaAsP, grown on an InP substrate by liquid phase epitaxy (LPE), have been examined with the rocking curve technique. Laser structures with multiple layers of differing alloy composition have been found to fail prematurely when the layer strains exceed a critical value. The solute concentrations of the elements Ga, As, and P are adjusted in the active layer (the Q 1 layer) to give the desired laser wavelength. Strains in a Q 1 layer which are coherent with the substrate may be larger than the critical value. Figure 5(a) shows a symmetric (004) rocking curve obtained from a single 5000-Å Q 1 layer. The positive $\Delta\theta$ of the layer peak indicates in-plane tensile stress in the Q 1 layer which would be detrimental to the performance of a laser structure. By growing several buffer layers of selected alloy content, a five-layer structure with strains below the critical value was made. The symmetric (004) rocking curve in Fig. 5(b) was obtained from the five-layer structure, and it indicates that

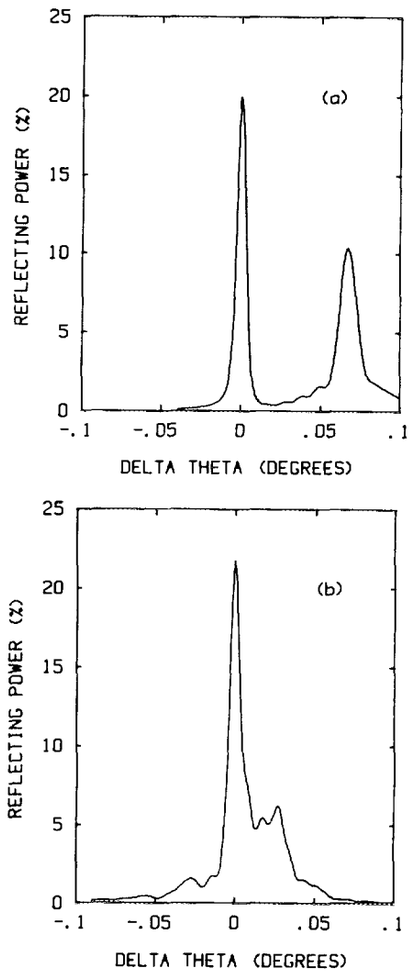

FIG. 5. (a) Fe $K_{\alpha 1}$ (004) symmetric rocking curve of a 5000-Å InGaAsP layer on an InP substrate. (b) Fe $K_{\alpha 1}$ (004) symmetric rocking curve of a five-layer laser structure with three layers of the same alloy composition as in (a). The smaller $\Delta\theta$ for the layer peaks in (b) indicates decoupling of the layers from the substrate.

the active Q 1 alloy layer is sufficiently decoupled from the InP substrate (by misfit dislocations) to significantly reduce its strain over that in Fig. 5(a).

D. Homoepitaxy: Si on Si

A rocking curve study of annealed (001) epitaxial Si grown on an (001) Si wafer, which had been implanted with 2.4×10^{18} O^+ ions/cm^2 at 550 °C, revealed that the epilayer was essentially strain-free but contained regions misoriented from the substrate by angles up to $\sim0.1°$.[12] A superimposed pair of symmetric (004) rocking curves from the sample (obtained by reversing the diffraction vectors) is shown in Fig. 6. The peak at $\Delta\theta = 0$ is from the Si substrate. The sum of $\Delta\theta$ for the two broad peaks from the epilayer is essentially zero, indicating zero perpendicular strain. The amplitude of the peaks was analyzed to find the net thickness of misoriented Si as a function of misorientation angle.

E. Superlattice structures

The periodic layer structure of superlattice produces periodic peaks and oscillations in the rocking curve which may be analyzed to determine the alloy content of the layers, the layer thicknesses, and in some cases the number of periods in the superlattice. The parameters (except for the numbers of periods) are often determined with significantly greater accuracy than the nominal parameters obtained from calibrations of the MOCVD, LPE, or molecular-beam epitaxy (MBE) growth systems.

Experimental and calculated symmetric (004) rocking curves for an AlSb/GaSb superlattice showing 14 distinct superlattice peaks[8] are shown in Fig. 7. Strains in each of the bilayers were determined. The superlattice was found to have lost some coherency with the substrate (parallel strain = 0.03%).

Rocking curves from MBE grown $Al_xGa_{1-x}As/GaAs$ superlattice structures with layer interface sharpness approaching atomic dimensions and high crystal perfection have been grown. An example is shown in Fig. 8, where in addition to the substrate peak at $\Delta\theta = 0$, the zero-order superlattice peak is seen.[13] The $\Delta\theta$ for this peak gives the average strain in the superlattice. The smaller periodic oscillations in the rocking curve have a wavelength which is directly proportional to the number of bilayer periods in the superlattice.[8]

X-ray rocking curves obtained from a HgCdTe/CdTe superlattice grown by laser MBE deposition were obtained and analyzed.[14] Experimental and calculated rocking curves are

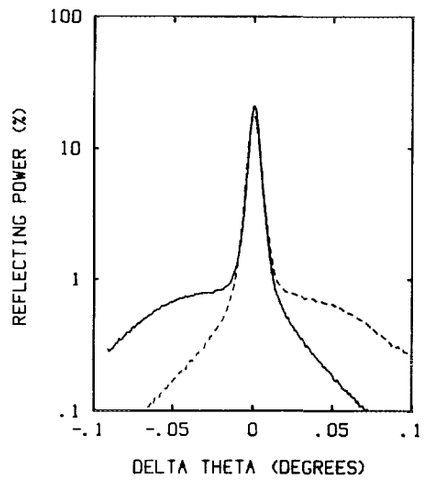

FIG. 6. Pair of superimposed symmetric (004) rocking curves from an (001) Si epilayer on Si using Fe $K_{\alpha1}$ with reversed diffraction vectors (Ref. 12). The Si was implanted with O^+ and annealed for 10 min in H_2 at 115 °C prior to growth of the epilayer at 1125 °C. The Si substrate peaks are at $\Delta\theta = 0$. The symmetric shifts of the broad layer peaks indicate misorientation of layer and substrate with essentially zero layer strain.

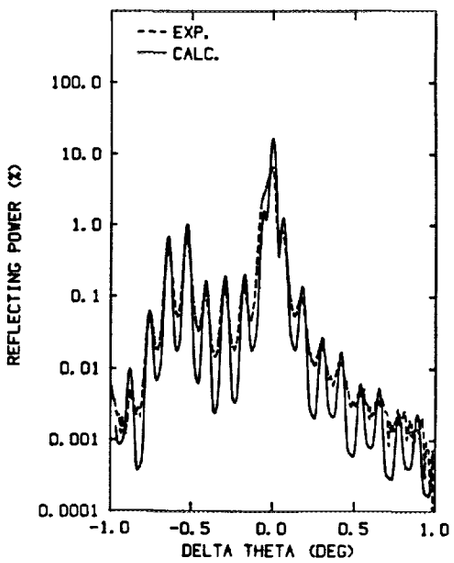

FIG. 7. Fe $K_{\alpha1}$ symmetric (004) rocking curves of an AlSb/GaSb superlattice (Ref. 7). The calculated curve is based on a bilayer period of 610 Å, with equal thickness layers of AlSb ($\epsilon^{\perp} = 1.25\%$) and GaSb ($\epsilon^{\perp} = -0.03\%$) and a parallel strain of 0.03% in all layers (Ref. 8).

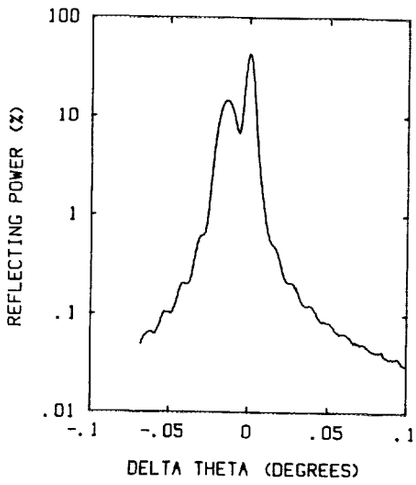

FIG. 8. Fe $K_{\alpha1}$ symmetric (004) rocking curve from an $Al_xGa_{1-x}As/GaAs$ superlattice showing the zero-order superlattice peak, in addition to the substrate peak at $\Delta\theta = 0$ (Ref. 13). The smaller periodic oscillations in the rocking curve have a wavelength which is directly proportional to the number of bilayer periods in the superlattice.

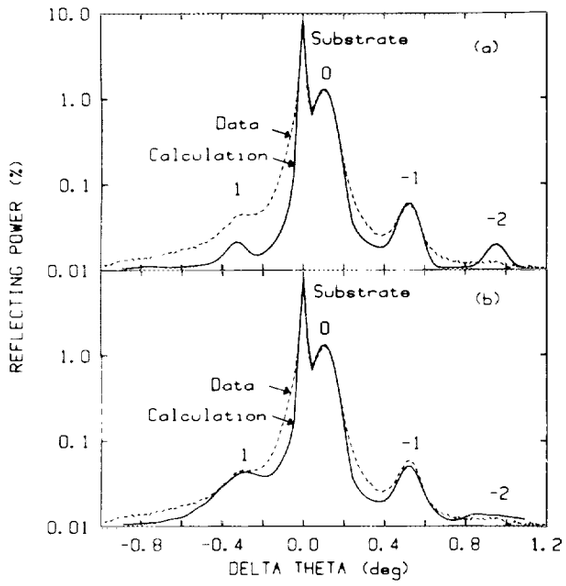

FIG. 9. Fe $K_{\alpha 1}$ symmetric (004) rocking curves of a HgTe/CdTe superlattice (Ref. 14) (a) with abrupt interfaces between layers, (b) with a strained region above the CdTe substrate and a 10% variation in thicknesses of the HgTe and CdTe layers. The numbers refer to the order of the superlattice peaks.

shown in Fig. 9. The calculated curve for a 14 period structure with abrupt interfaces is shown in Fig. 9(a), while the better fit in Fig. 9(b) is obtained with a calculation which assumed a narrow strained region above the CdTe substrate, and 10% variations in the thickness of the HgTe and CdTe layers (or intermixed regions between layers on the order of 10% of the layer thicknesses).

F. Ion implanted crystals

Strain can be induced in single crystals by ion implantation. Profiles of strain with depth have been measured for Si,[15,16] magnetic garnet,[17] and GaAs.[5,18–21]

Figure 10(a) shows experimental and calculated rocking curves for GaAs after an implantation of 300 keV Si^+ ions to a dose of 1×10^{13} ions/cm^2. The solid calculated curve was obtained for the layer approximation to a continuous strain distribution shown by the stepped curve in Fig. 10(b). The continuous curve in Fig. 10(b) is the profile of energy per unit depth deposited in nuclear collisions, denoted by F_D (calculated with a Monte Carlo simulation). The very close correspondence of the two curves is strong evidence that the ion-induced strain is directly related to atomic displacements caused by nuclear collisions.[20]

Rocking curves for GaAs after implantation of 15 MeV Cl^{+4} ions to a dose of 5×10^{15}/cm^2 are shown in Fig. 11(a).[18] The strain (solid) and damage (dashed) profiles which gave the calculated curve are shown in Fig. 11(b). The damage was modeled as a spherically symmetric Gaussian displacement of atoms from normal lattice sites, with the standard deviation plotted in Fig. 11(b). Here, because of the greater penetration of the ions, a thick damage layer is formed, and the dynamical model was used for analysis. The large strain peak in Fig. 11(a) indicates that the strained

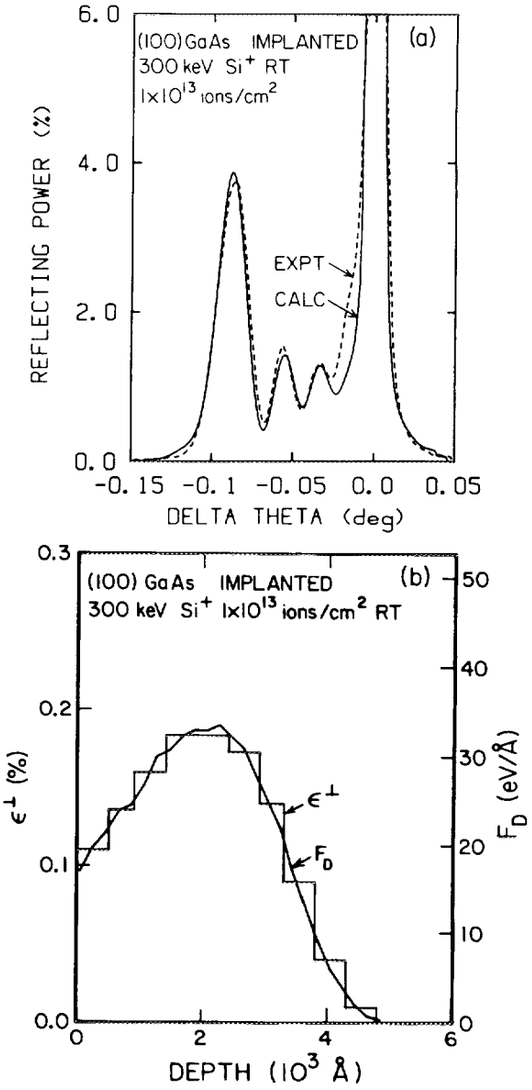

FIG. 10. (a) Experimental and calculated Fe $K_{\alpha 1}$ (004) rocking curves for GaAs after an implantation of 300 keV Si^+ to a dose of 1×10^{13} ions/cm^2. The calculated curve was obtained using the perpendicular x-ray strain vs depth profile shown in (b). The calculated ion energy per angstrom lost to nuclear collisions vs depth is also plotted in (b) (Ref. 20).

layer is thick and has relatively constant strain with depth. The substrate peak is weak because of absorption in the thick damaged layer. An amorphous layer is formed beneath the thick strained layer (damage ~0.44 Å). Rocking curve studies of strain saturation effects and the role of nuclear and electronic collisions are given in Refs. 18, 20, and 21, and thermal annealing of strain in GaAs and GaP was treated in Ref. 19.

X-ray rocking curves were utilized in a study of Si^+ ion implantation into an AlGaAs/GaAs superlattice.[22] The implantation significantly altered the average strain in the superlattice as well as the difference between the strains in the alternating layers. It was demonstrated that the implantation strains are removed by a 1-h anneal at 420 °C. The rocking curve of the annealed sample is essentially the same as the rocking curve obtained from the as-grown superlattice, indicating that intermixing of the layers was negligible.

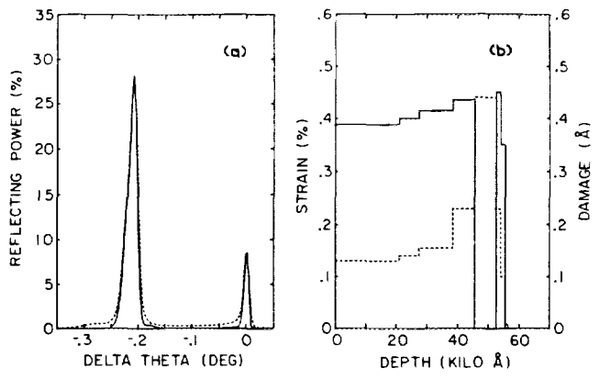

FIG. 11. (a) Experimental (dashed) and calculated (solid) Fe $K_{\alpha 1}$ (004) rocking curves for GaAs after implantation of 15 MeV Cl^{+4} to a dose of 5×10^{15} ions/cm^2 (Ref. 5). The calculated curve was obtained using the depth profiles of strain (solid) and damage (dashed) shown in (b). The high damage region (4.5–5.8 kÅ in depth) has a very small structure factor (corresponding to an amorphous structure), so strain in this region cannot be obtained from the rocking curve.

G. Strains in polycrystalline or noncrystalline films on thin single crystals

Sensitive measurements of the lattice curvature of crystals are possible using the rocking curve system. The shift of a Bragg peak with position over the surface of a laterally uniform crystal is measured from which lattice curvature is obtained. Crystal radii of curvature in excess of 1 km are detected (in high-quality crystals). A study of the stresses in evaporated metal layers on Si crystals is in progress. Of interest in this study are the stress changes which accompany solid-state reactions in the metal layers.

ACKNOWLEDGMENTS

The rocking curve work at Caltech was initiated by Dr. V. S. Speriosu, now with the IBM Almaden Research Laboratory, San Jose, CA. Our rocking curve system was designed and built with DARPA support. Research support has been provided by DARPA (MDA 903-82-C-0348), NSF (DMR 83-18274 and DMR 84-21119), and the Semiconductor Research Corporation (No. 85-04-059). The authors wish to thank Dr. Speriosu for introducing this technique to them, and the supporting agencies which made this work possible.

[1]U. Bonse and I. Hartmann, Z. Kristallogr. **156**, 256 (1981).
[2]V. S. Speriosu, J. Appl. Phys. **52**, 6094 (1981).
[3]S. Takagi, Acta Cryst. **15**, 1311 (1962); D. Taupin, Bull. Soc. Franc. Miner. Cryst. **87**, 469 (1964).
[4]W. J. Bartels, J. Vac. Sci. Technol. B **1**, 338 (1983).
[5]C. R. Wie, T. A. Tombrello, and T. Vreeland, Jr., J. Appl. Phys. **59**, 3743 (1986).
[6]M. Wilkens, Phys. Status Solidi A **2**, 359 (1970).
[7]U. Bonse, Z. Physik **153**, 278 (1958).
[8]V. S. Speriosu and T. Vreeland, Jr., J. Appl. Phys. **56**, 159 (1984).
[9]V. S. Speriosu, M.-A. Nicolet, J. L. Tandon, and Y. C. M. Yeh, J. Appl. Phys. **57**, 1377 (1985).
[10]A. H. Hamdi, M.-A. Nicolet, Y. C. Kao, M. Tejwani, and K. C. Wang, in *Materials Research Society Proceedings* (Materials Research Society, Pittsburgh, PA, 1985), Vol. 41, p. 355.
[11]T. Vreeland, Jr., J. Mater. Res. (to be published).
[12]T. Vreeland, Jr. and T. S. Jayadev, *Materials Research Society Symposium Proceedings* (Materials Research Society, Pittsburgh, PA, in press), Vol. 56.
[13]T. Vreeland, Jr. (unpublished).
[14]B. M. Paine, T. Vreeland, Jr., and J. T. Cheung, Mater. Res. Soc. Symp. Proc. **56** (in press).
[15]F. Cembali, A. M. Mazzone, and M. Servidori, Phys. Status Solidi A **91**, K125 (1985).
[16]V. D. Tkachev, G. Holzer, and A. R. Chelyadinskii, Phys. Status Solidi A **85**, K43 (1984).
[17]B. E. MacNeal and V. S. Speriosu, J. Appl. Phys. **52**, 3935 (1981).
[18]C. R. Wie, T. A. Tombrello, and T. Vreeland, Jr., Phys. Rev. B **33**, 4083 (1986).
[19]C. R. Wei, T. Vreeland, Jr., and T. A. Tombrello, Nucl. Instrum. Methods **B16**, 44 (1986).
[20]B. M. Paine, M. M. Hurvitz, and V. S. Speriosu, J. Appl. Phys. (in press).
[21]B. M. Paine, V. S. Speriosu, and M. M. Hurvitz (unpublished).
[22]A. H. Hamdi, J. L. Tandon, T. Vreeland, Jr., and M.-A. Nicolet, Mater. Res. Soc. Symp. Proc. **37**, 319 (1985).